

Journal of
Mechanics of
Materials and Structures

**DYNAMIC RIGID-PLASTIC DEFORMATION OF ARBITRARILY
SHAPED PLATES**

Tatiana Pavlovna Romanova and Yuri Vladimirovich Nemirovsky

Volume 3, N° 2

February 2008



mathematical sciences publishers

DYNAMIC RIGID-PLASTIC DEFORMATION OF ARBITRARILY SHAPED PLATES

TATIANA PAVLOVNA ROMANOVA AND YURI VLADIMIROVICH NEMIROVSKY

A rigid, perfectly-plastic model of solids is applied to study the dynamic behavior of simply supported or clamped, arbitrarily shaped plates on visco-elastic foundation. The role of membrane forces and transverse shear forces in the yield condition and the influence of geometry changes are neglected. The plate is subjected to explosive loads uniformly distributed over the surface. Several mechanisms of dynamic deformation of the plate are considered. For each mechanism, equations of the dynamic behavior are obtained. Operating conditions of these mechanisms are analyzed. Analytical expressions for the limit and high loads and for the maximum final deflections are obtained. Detailed analyses are given for an astroid-shaped plate, for a plate with a contour consisting of two arcs and for a plate with an internal free hole or a rigid insert.

1. Introduction

The issues involved in calculating structural deformation under the action of intensive short-time loads are important in modern solid mechanics. To solve such problems, the model of a rigid-plastic body is widely used [Komarov and Nemirovsky 1984]. The model is based on the assumption that the body starts deforming if the stress reaches the limiting value and plastic deformations become possible. Elastic deformations are neglected. For thin-walled elements of structures, this simplification allows solving numerous important practical problems. Nevertheless, all well-known solutions concern only axisymmetric and rectangular plates.

The method proposed in the present work allows, on the basis of the theory of a rigid, perfectly-plastic body, calculating any supported plates of an arbitrary piecewise smooth curvilinear contour, subjected to short-time intensive dynamic loads. The method can be useful in engineering practice.

Notation

P	intensity of load
P_{\max}	maximum value of load
P_0, \bar{P}_0	limit loads
P_1	load defining high loads
p_0, p_1, P_m	dimensionless loads
t, t_0	current and initial times
K_1, K_2	factors of elastic and viscous resistance

Keywords: rigid-plastic plate, arbitrarily shaped plate, dynamic load, limit load, final deflection.

This work was supported by the Russian Foundation for Basic Research (grant no. 05-01-00161-a).

Z_1, Z_2, S_p	regions in plate
l	contour of plate
dl	element of contour l
l_1, l_2	plastic hinge curves
$(x, y), (x_1, y_1),$ $(x_2, y_2), (x_h, y_h)$	Cartesian coordinates
φ, φ_h	parameters
$\varphi_i, \varphi_j, \varphi_D, \varphi_{hi}, \varphi^b, \varphi_h^b$	boundary values of parameter φ
φ_0	initial value of parameter φ_D
$D_h, D_{\min}, D_{\max}, D,$ D_0, D_a, d_i, d_1, d_2	distances
K, A, N	powers of inertial, external and internal forces
S	area of plate
ds	element of area
u, w_c	deflections
w_{\max}	maximum of final deflection
ρ, ρ_a	surface density of plate material and insert material
l_m	lines of discontinuity of angular velocity
m	quantity of lines of discontinuity of angular velocities
$[\partial\theta_m/\partial t]$	discontinuity of angular velocities on l_m
dl_m	element of line l_m
κ_1, κ_2	main curvatures of surface of deflection rate of plate
$\dot{\alpha}$	rate of change of angle of rotation
*	index denoting admissible velocities
M_m	bending moment on l_m
M_0	limit bending moment
n	normal to the contour l
AB, AC	normals to the contour l
η	parameter of supported contour
β	parameter of internal contour
i, j	indexes
(v_1, v_2)	curvilinear orthogonal coordinates
v_{2h}	parameter corresponding to v_2
v_{2j}	boundary value of parameter v_2
a_1, b_1	semiaxes of semiellipse
a	parameter of astroid-shaped plate
L	function designated in Equation (2)
L_h	function designated in Equation (15)
$\Sigma_1, \Sigma_2, \Sigma_3, \Sigma_4, \Sigma_5, \Sigma_6, G, G_1, F$	factors
T	time of removing of load
t_1	time of end of first phase of deformation
t_f	time of stop of plate

R, γ	radius and half of central corner of arc of circle
I, I_*	integral characteristics of load
\bar{l}, \bar{l}_2	polygonal contours
δ, δ_0	dimensionless functions
r	radius of curvature of curve l
r_1	radius
ξ, ς	coordinates of center of curvature of curve l
ρ_1, ρ_2	radiuses of curvature
N_1, N_2, N_3, N_4	components of power of internal forces in plate
l_3	tangent to curve l_1
ABE, BED_1, AED_1, AD_2E	planes
$\psi_1, \psi_2, \beta_1, \beta_2$	angles in Figure 3

2. Model, assumptions and equations of motion

We consider a thin rigid perfectly-plastic simply supported or clamped plate of an arbitrary piecewise smooth curvilinear contour l (Figure 1). The plate is subjected to a uniformly distributed short-time intensive dynamic load of high intensity $P(t)$. We consider explosive load characterized by the instantaneous reaching of the maximum value $P_{\max} = P(t_0)$ at the initial time t_0 with the subsequent rapid decrease. The plate rests on a viscoelastic foundation (K_1 and K_2 are the coefficients of elastic and viscous resistance). The deflections are small. The role of membrane forces and transverse shear forces in the yield condition and the influence of geometry changes are ignored.

Let the equations for the contour l of the plate be written in a parametric form

$$x = x_1(\varphi), \quad y = y_1(\varphi), \quad \text{with } 0 \leq \varphi \leq 2\pi.$$

Except for singular points, the radius of curvature of the contour l is equal to

$$r(\varphi) = \frac{L^3}{x_1' y_1'' - y_1' x_1''}, \quad (1)$$

$$L(\varphi) = \sqrt{x_1'^2(\varphi) + y_1'^2(\varphi)}, \quad (\cdot)' = \partial(\cdot)/\partial\varphi. \quad (2)$$

To be specific, we assume that the x -size of the plate is not smaller than its geometric size along the y axis. We have two assumptions about the shape of the deformable plate.

Assumption 1. Under the loads slightly higher than the limit load P_0 , a plastic hinge line l_1 is formed in the internal area of the plate (Figure 1). As a result, the plate is deformed into parts of certain ruled surfaces. The normal bending moment on the line l_1 is equal to the limit bending moment M_0 . The line l_1 can consist of several parts (Figure 1 bottom) or degenerate into a point (for a circular plate). The parts of the plastic hinge line l_1 can be either rectilinear or curvilinear. If there are singular points on the contour l then the line l_1 intersects them (the top left and bottom of Figure 1).

We assume that the rate of variation of the angle of plate-surface rotation with respect to the horizontal plane at the contour l is independent of the parameter φ and that the position of the line l_1 is determined

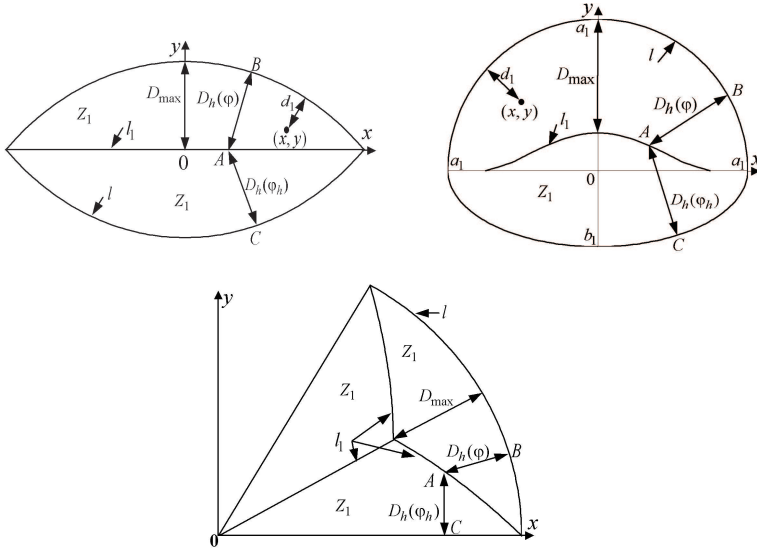


Figure 1. Mechanism 1 for the plates of different shapes.

from the condition of equality of the distances measured along the normal to the external contour l from the line l_1 to the contour l . This assumption is substantiated for a sector plate by Nemirovsky and Romanova [2004], based on the condition of minimum of the limit load. This assumption is obviously valid for a circular plate [Hopkins and Prager 1953].

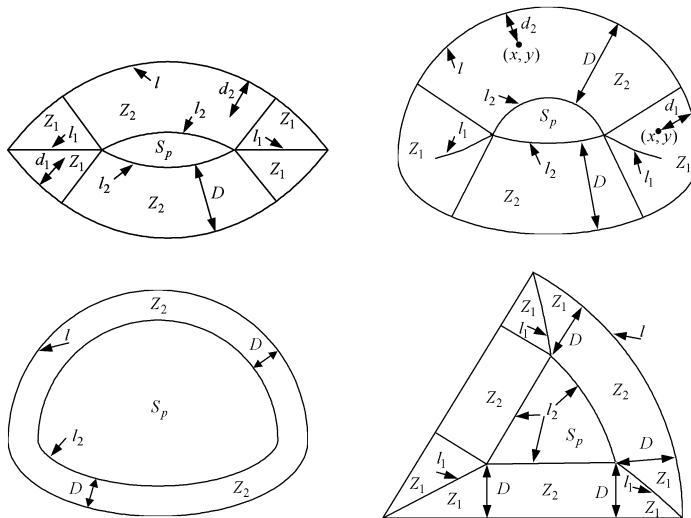


Figure 2. Mechanism 2 and 3 for the plates of different shapes (the positions of the coordinate axes are the same as those in Figure 1).

Assumption 2. Under rather high loads, a region S_p of an intense plastic deformation is formed in the internal area of the plate (Figure 2). The region S_p moves translationally. The contour of the region S_p is the plastic hinge line l_2 , and the normal bending moment on the line l_2 is equal to M_0 .

Let the equations for the line l_1 have the form $x = x_h(\varphi)$, $y = y_h(\varphi)$. The distance D_h measured along the normal to the contour l from the line l to l_1 is

$$D_h(\varphi) = \sqrt{[x_1(\varphi) - x_h(\varphi)]^2 + [y_1(\varphi) - y_h(\varphi)]^2}. \quad (3)$$

From the Assumption 1, it follows that the line l_1 is defined by the system of equations

$$\begin{aligned} x'_1(\varphi)[x_h(\varphi) - x_1(\varphi)] + y'_1(\varphi)[y_h(\varphi) - y_1(\varphi)] &= 0, \\ x'_1(\varphi_h)[x_h(\varphi) - x_1(\varphi_h)] + y'_1(\varphi_h)[y_h(\varphi) - y_1(\varphi_h)] &= 0, \\ D_h(\varphi) = D_h(\varphi_h), \quad x_h(\varphi) = x_h(\varphi_h), \quad y_h(\varphi) = y_h(\varphi_h). \end{aligned} \quad (4)$$

Here φ_h corresponds to φ parameter of the contour l , for which the relation $|AB| = |AC|$ holds (AB , AC are the perpendiculars to the contour l in Figure 1). The plates of different shapes and the positions of the lines l_1 in the plates are presented in Figure 1.

The normal to the contour curve l directed inward the region occupied by the plate gets either on the line l_1 , or on the line l_2 : $x = x_2(\varphi)$, $y = y_2(\varphi)$. We denote by Z_i the region of the plate that does not involve the region S_p in which the normal from any point to the contour l gets on the line l_i for $i = 1, 2$ (Figures 1–2). The number of the regions Z_i depends on the shape of the support counter l of the plate. In Appendix A, it is shown that the normal to the curve l_2 is also the normal to the contour l . In Appendix B, it is shown that, in any smooth part of the contour l , the distance between curves l_2 and l is independent of the parameter φ and the equation for the curve l_2 looks like Equation (B.5) if the region S_p is nonsingular. From the definition of the line l_1 , it follows that at the boundaries of the regions Z_1 and Z_2 the relations $D(t) = D_h(\varphi^b(t)) = D_h(\varphi_h^b(t))$ where φ^b , φ_h^b are the parameters of the boundaries of the regions Z_1 and Z_2 . Consequently, the distance between curves l_2 and l in all regions Z_2 is the same and is equal to $D(t)$ (Figure 2).

Depending on the value of P_{\max} , three mechanisms of deformation are possible in the dynamics of a rigid-plastic plate. Under the loads lower than the limit load (low loads, $0 < P_{\max} \leq P_0$), the plate remains at rest. For the loads slightly higher than the limit load (moderate loads, $P_0 < P_{\max} \leq P_1$) as in the cases of a bending of beams [Mazalov and Nemirovsky 1975; Komarov and Nemirovsky 1984], circular and annular plates [Hopkins and Prager 1953; 1954; Perzyna 1958; Florence 1965; 1966; Youngdahl 1971], rectangular and polygonal plates [Jones et al. 1970; Virma 1972; Mazalov and Nemirovsky 1975; Nemirovsky and Romanova 1987; 1988], the plastic hinge line l_1 is formed in the internal area of the plate (see Assumption 1). Let us call this mechanism of deformation *mechanism 1* (Figure 1). For the values of P_{\max} ($P_{\max} > P_1$) high enough, the dynamics of the plate as the dynamics of all above-listed structures yields the emergence of the intense plastic deformation region S_p that moves translationally (see Assumption 2). Thus, two situations are possible: that the line l_1 is present (*mechanism 2* is presented in the top left, top right and the bottom right of Figure 2 for high loads) and that the line l_1 does not present (*mechanism 3* is presented in the bottom left of Figure 2 for super high loads).

Let us denote

$$\max_{\varphi} D_h(\varphi) = D_{\max} \quad \text{and} \quad \min_{\varphi} D_h(\varphi) = D_{\min}.$$

For the curve l_2 that has no mutually intersected segments, the following conditions must be satisfied.

$$D < D_{\max} \quad \text{and} \quad y_2(\varphi) \geq y_h(\varphi), \quad y_2(\varphi_h) \leq y_h(\varphi_h),$$

(see the plates presented in the top left and top right of Figure 2 for example). Therefore, the curve l_2 presented in (B.5) is not determined for all values of φ . The case $D \geq D_{\max}$ corresponds to mechanism 1 that the region S_p and the curve l_2 are absent (Figure 1); the case $D_{\min} \leq D < D_{\max}$ corresponds to mechanism 2 (top left, top right and the bottom right of Figure 2); the case $D < D_{\min}$ corresponds to mechanism 3. For the plates with singular points on the supporting contour l , equality $D_{\min} = 0$ carries out. Therefore, such plates are not deformed according to mechanism 3 (Figure 2, top left and bottom right) and they have plastic hinge line l_1 present in deformation with any action of the loads exceeding the the limit load. Mechanism 3 is realized only for plates with a smooth contour l (Figure 2, bottom left).

Mechanism 2 corresponds to a general case of deformation of the plate. In the absence of the region S_p , it corresponds to mechanism 1. If the line l_1 is absent then it corresponds to mechanism 3. Let us consider mechanism 2 in detail.

According to mechanism 2, the equations of motion of the plate, that we obtain from the virtual power principle and d’Alembert principle [Erkhov 1978], are

$$K = A - N, \tag{5}$$

$$K = \iint_S \rho \frac{\partial^2 u}{\partial t^2} \frac{\partial u^*}{\partial t} ds, \quad A = \iint_S \left[P(t) - K_1 u - K_2 \frac{\partial u}{\partial t} \right] \frac{\partial u^*}{\partial t} ds, \tag{6}$$

$$N = \sum_m \int_{l_m} M_m \left[\frac{\partial \theta^*}{\partial t} \right]_{l_m} dl_m + M_0 \iint_S (|\kappa_1^*| + |\kappa_2^*|) ds. \tag{7}$$

Here K , A , N are the powers of inertial, external and internal forces in the plate, respectively; S is the area of the plate; u is the deflection; ρ is the surface density of the plate material; t is the current time; ds is the element of area of the plate; m is the index of the lines of discontinuity of angular velocity; l_m are the lines of discontinuity in angular velocity including the contour of the plate; $[\partial \theta / \partial t]_{l_m}$ is the discontinuity in angular velocity on l_m ; M_m is the bending moment on l_m ; dl_m is the element of line for l_m ; κ_1 and κ_2 are the main curvatures of surface of deflection rate of plate. The upper index “*” denotes the admissible velocities. If there is no resistance foundation, Equation (5) coincides with the equation of motion of [Jones 1971a], the axial forces being assumed to equal zero, which means that geometrical changes are ignored. Note that Jones [1971a] suggests using this equation for plates of an arbitrary contour and arbitrary edge conditions; however, it has been used in the literature up to now for circular and rectangular plates only [Jones 1971b; Jones and Shen 1993; Jones 1973; Zhu et al. 1994].

Let us denote the deflection and the velocity of the deflection in the region S_p by $w_c(t)$ and $\dot{w}_c(t)$, where $\dot{f} = \partial f / \partial t$ for function f . Let us denote the angle of rotation of the region Z_2 from the horizontal plane at the supported contour by α . Because of the continuity of velocities at the boundaries of the regions S_p and Z_2 , the rate of variation of this angle α is independent of the parameter φ . Taking into

account of the continuity of velocities at the boundary of the regions Z_1 and Z_2 and Assumption 1, we obtain that the rate of variation of the angle of rotation of the region Z_1 at the supported contour is equal to $\dot{\alpha}(t)$. The deflection rate in the different regions of the plate is given by

$$\begin{aligned} (x, y) \in Z_i &: \dot{u}(x, y, t) = \dot{\alpha}(t)d_i(x, y), \quad i = 1, 2, \\ (x, y) \in S_p &: \dot{u}(x, y, t) = \dot{w}_c(t), \end{aligned} \tag{8}$$

where $d_i(x, y)$ is the distance from a point (x, y) to the supported contour of the region Z_i (Figure 1–2).

We introduce the curvilinear orthogonal coordinate system (v_1, v_2) related to the Cartesian coordinate system by the relations

$$x = x_1(v_2) - v_1 \frac{y'_1(v_2)}{L(v_2)}, \quad y = y_1(v_2) + v_1 \frac{x'_1(v_2)}{L(v_2)}. \tag{9}$$

The curves $v_1 = \text{const}$ are at the distance v_1 from the contour l and have the radius of the curvature $\rho_1 = r(v_2) - v_1$. The straight lines $v_2 = \text{const}$ are the perpendiculars to the external contour l of the plate. Their radius of the curvature is $\rho_2 = \infty$. The element of area is $ds = L(1 - v_1/r)dv_1dv_2$. Then the equation of the supported contour l has the form $v_1 = 0$ for $0 \leq v_2 \leq 2\pi$. If the line l_1 consists of one part then its equation has the form $v_1 = D_h(v_2)$ for $0 \leq v_2 \leq \varphi_1$, $\varphi_2 \leq v_2 \leq \pi$. The equation of the line l_2 has the form $v_1 = D(t)$ for $\varphi_1 \leq v_2 \leq \varphi_2$, $\varphi_{h2} \leq v_2 \leq \varphi_{h1}$ where, for $i = 1, 2$, φ_i, φ_{hi} are boundary values.

Then the deflection rate of the plate (8) is given by:

$$\begin{aligned} (x, y) \in Z_i &: \dot{u}(v_1, v_2, t) = \dot{\alpha}(t)v_1, \quad i = 1, 2, \\ (x, y) \in S_p &: \dot{u}(v_1, v_2, t) = \dot{w}_c(t). \end{aligned} \tag{10}$$

With the introduced denotations and (10) taken into account, the expressions (6) become

$$\begin{aligned} K &= \rho \left[\dot{\alpha}^* \ddot{\alpha} \sum_{i=1}^2 \iint_{Z_i} v_1^2 ds + \dot{w}_c^* \ddot{w}_c \iint_{S_p} ds \right], \\ A &= \dot{\alpha}^* \sum_{i=1}^2 \iint_{Z_i} [P(t) - K_1 \alpha v_1 - K_2 \dot{\alpha} v_1] v_1 ds + \dot{w}_c^* \iint_{S_p} [P(t) - K_1 w_c - K_2 \dot{w}_c] ds. \end{aligned} \tag{11}$$

We represent the expression (7) for the power of internal forces in the plate in the form

$$N = \sum_{i=1}^4 N_i \tag{12}$$

where N_1, N_2, N_3, N_4 are the powers of internal forces on the contour l , in the regions Z_1 and Z_2 , on the line l_2 and on the line l_1 , respectively:

$$\begin{aligned} N_1 &= (1 - \eta)M_0 \oint_l [\dot{\theta}^*]_l dl, & N_2 &= M_0 \iint_{Z_1 \cup Z_2} (|\kappa_1^*| + |\kappa_2^*|) ds, \\ N_3 &= M_0 \oint_{l_2} [\dot{\theta}^*]_{l_2} dl_2, & N_4 &= M_0 \int_{l_1} [\dot{\theta}^*]_{l_1} dl_1. \end{aligned} \tag{13}$$

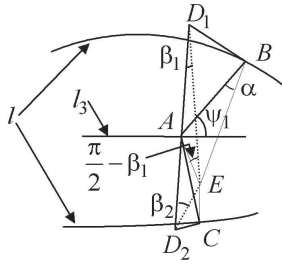


Figure 3. Supplementary construction for the calculation of the discontinuity of angular velocity on l_1 .

Here $\eta = 0$ for the clamped contour l and $\eta = 1$ for the simply supported contour.

From (10) and the normal to the line l_2 is the normal to the contour l , it follows that

$$[\dot{\theta}^*]_{l_1} = [\dot{\theta}^*]_{l_2} = \dot{\alpha}, \quad \kappa_1 = \frac{\partial^2 \dot{u}}{\partial v_1^2} = 0, \quad \kappa_2 = \frac{1}{\rho_1} \frac{\partial \dot{u}}{\partial v_1} = \frac{\dot{\alpha}(t)}{r - v_1}.$$

Then we have

$$N_1 = (1 - \eta) M_0 \dot{\alpha}^* \int_0^{2\pi} L dv_2,$$

$$N_2 = M_0 \dot{\alpha}^* \iint_{Z_1 \cup Z_2} \frac{1}{r - v_1} ds$$

$$= M_0 \dot{\alpha}^* \left[\int_0^{\varphi_1} \frac{L D_h}{r} dv_2 + \left(\int_{\varphi_1}^{\varphi_2} \frac{L}{r} dv_2 \right) D(t) + \int_{\varphi_2}^{\varphi_{h2}} \frac{L D_h}{r} dv_2 + \left(\int_{2\pi - \varphi_{h2}}^{2\pi - \varphi_{h1}} \frac{L}{r} dv_2 \right) D(t) + \int_{\varphi_{h1}}^{2\pi} \frac{L D_h}{r} dv_2 \right], \tag{14}$$

$$N_3 = M_0 \dot{\alpha}^* \oint_{l_2} dl_2 = M_0 \dot{\alpha}^* \left\{ \int_{\varphi_1}^{\varphi_2} L \left[1 - \frac{D(t)}{r} \right] dv_2 + \int_{\varphi_{h2}}^{\varphi_{h1}} L \left[1 - \frac{D(t)}{r} \right] dv_2 \right\}.$$

To calculate N_4 in (13), we have

$$dl_1 = L_h dv_2, \quad \text{where } L_h = \sqrt{x_h'^2 + y_h'^2}. \tag{15}$$

We consider a case where the line l_1 consists of one part. For the calculation of $[\dot{\theta}^*]_{l_1}$ with $v_2 \in [0, \varphi_1]$ at point $A = (D_h(v_2), v_2) \in l_1$ of the undeformed plate, we draw the perpendiculars AB and AC that they intersect the contour l at $B = (0, v_2)$ and $C = (0, v_{2h})$ so $AB \perp l$, $AC \perp l$, $|AB| = |AC| = D_h(v_2)$ (Figure 1, 3). At point A , we draw the line l_3 which is tangent to the line l_1 . Through the segment AB , we draw the plane ABE which is perpendicular to an initial surface of the plate, where $AE \perp AB$ (Figure 3). We draw the plane BED_1 which is tangent to the deformed surface of the plate along the straight line BE . Then we have $\angle ABE = \alpha$. Through point B , we draw the plane AED_1 which is perpendicular to the line l_3 . Let us denote $\angle AD_1E = \beta_1$. With the similar constructions for point C , we obtain point

D_2 such that the equality $\angle AD_2E = \beta_2$ holds. Then we have $[\dot{\theta}^*]_{l_1}(v_2) = \dot{\beta}_1 + \dot{\beta}_2$. From $|AE| = |AB|\alpha$, $|AE| = |AD_1|\beta_1$ and $AB \perp BD_1$, it follows that

$$\dot{\beta}_1 = \dot{\alpha} \sin \psi_1, \tag{16}$$

where ψ_1 is the minimum angle between the segment AB and the line l_3 such that

$$\sin \psi_1 = \frac{y'_1 y'_h + x'_1 x'_h}{LL_h}. \tag{17}$$

In a similar manner, $\dot{\beta}_2 = \dot{\alpha} \sin \psi_2$ where ψ_2 is the minimum angle between the segment AC and the line l_3 . From (15)–(17), it follows that

$$\dot{\beta}_1 dl_1 = \dot{\alpha} \frac{y'_1 y'_h + x'_1 x'_h}{L} dv_2.$$

From (1), (3), (4), it follows that

$$\frac{y'_1 y'_h + x'_1 x'_h}{L} = L \left[1 - \frac{D_h(v_2)}{r} \right];$$

then we have

$$\dot{\beta}_1 dl_1 = \dot{\alpha} L \left[1 - \frac{D_h(v_2)}{r} \right] dv_2 \quad \text{for } v_2 \in [0, \varphi_1].$$

In a like manner, we obtain

$$\dot{\beta}_2 dl_1 = \dot{\alpha} L \left[1 - \frac{D_h(v_2)}{r} \right] dv_2 \quad \text{for } v_2 \in [\varphi_{h1}, 2\pi].$$

We have similar expression for $v_2 \in [\varphi_2, \pi]$ and $v_2 \in [\pi, \varphi_{h2}]$. Then the expression (13) for N_4 looks like

$$N_4 = M_0 \dot{\alpha}^* \left[\int_0^{\varphi_1} L \left(1 - \frac{D_h}{r} \right) dv_2 + \int_{\varphi_2}^{\varphi_{h2}} L \left(1 - \frac{D_h}{r} \right) dv_2 + \int_{\varphi_{h1}}^{2\pi} L \left(1 - \frac{D_h}{r} \right) dv_2 \right]. \tag{18}$$

Substituting the expressions (14), (18) into (12), we get the power of internal forces in the plate

$$N = M_0(2 - \eta) \dot{\alpha}^* \int_l dl. \tag{19}$$

The expression (19) for the cases of smooth or pyramidal shape of the deformable plate coincides with the result obtained by Rzhantsyn [1982]. It is possible to show that the expression (7) for the power of internal forces has the form (19) also in the case that the line l_1 consists of several parts.

Substituting equalities (11), (19) into (5) and taking into account that $\dot{w}_c^*(t)$ and $\dot{\alpha}^*(t)$ are independent, we obtain the following equations of motion

$$(\rho \ddot{\alpha} + K_2 \dot{\alpha} + K_1 \alpha) \sum_i \iint_{Z_i} v_1^2 ds = P(t) \sum_i \iint_{Z_i} v_1 ds - M_0(2 - \eta) \int_l dl, \quad (i = 1, 2) \tag{20}$$

$$\rho \ddot{w}_c + K_2 \dot{w}_c + K_1 w_c = P(t). \tag{21}$$

The condition of the continuity of velocities at the boundaries of the regions S_p and Z_2 yields the equality

$$\dot{\alpha}D = \dot{w}_c. \quad (22)$$

At the boundaries of the regions Z_1 and Z_2 , we have the following relations

$$D = D_h(v_{2j}) \quad (23)$$

where $j = 1, \dots$ and $v_{2j}(t)$ are the parameters of the boundaries of the regions Z_1 and Z_2 .

At the initial time, the plate is at rest and undeformed as

$$\alpha(t_0) = \dot{\alpha}(t_0) = w_c(t_0) = \dot{w}_c(t_0) = 0. \quad (24)$$

The initial value $D_0 = D(t_0)$ depends on the value of P_{\max} . This is shown below for some special cases.

The system of Equations (20)–(23), for $i = 1, 2$ describes the plate motion according to mechanism 2. In the case of deformation according to mechanism 1, the regions S_p and Z_2 are absent and the plate motion is described by Equation (20) for $i = 1$. In the case of deformation according to mechanism 3, the region Z_1 does not present and the behavior of the plate is governed by Equations (20)–(22) for $i = 2$.

The method described in the present work is used to study the dynamic behavior of the following plates in the absence of resistance foundation: elliptical plates [Nemirovsky and Romanova 2002a], a plate with a contour consisting of a semicircle of radius a_1 and a semiellipse with semiaxes a_1 and b_1 with $b_1 \leq a_1$ (the top right of Figure 1, the top right, bottom left of Figure 2) [Nemirovsky and Romanova 2002b], a plate with a contour consisting of straight-line and arbitrary smooth curvilinear parts [Nemirovsky and Romanova 2002c], a plate with a contour consisting of two semicircles and two straight-line segments [Nemirovsky and Romanova 2001b], sector plates [Nemirovsky and Romanova 2004] (the bottom of Figure 1 and the bottom right of Figure 2).

Below we consider the examples of the dynamic behavior of plates of an arbitrary contour in the absent of visco-elastic foundation. The method proposed in the present work allows to take into account resistance foundation. The influence of visco-elastic foundation on final deflections and the opportunity of the optimization of the process of pulsed forming of metal plates of sophisticated contour were discussed by Nemirovsky and Romanova [1991; 2001a].

3. Dynamic behavior of a rigid-plastic astroid-shaped plate

We consider the dynamic behavior of the plates of an arbitrary contour by an example of the astroid-shaped plate whose contour is written in a parametric form $x_1 = a \cos^3 \varphi$ and $y_1 = a \sin^3 \varphi$ with $0 \leq \varphi \leq 2\pi$ (Figure 4 left). For this plate, we have

$$L(\varphi) = 3a|\sin \varphi \cos \varphi|, \quad D_h(\varphi) = a|\sin^3 \varphi / \cos \varphi|, \quad D_{\max} = D_h(\pi/4) = a/2.$$

Depending on the value of P_{\max} , two mechanisms of deformation are possible for the plate being considered. Under moderate loads, the plate is deformed into four parts of a ruled surface with the formation of four rectilinear plastic hinge lines located on the coordinate axes (mechanism 1 is presented in Figure 4, left). Under high loads, the region S_p is formed in the central part of the plate. The region S_p moves translationally (mechanism 2 is presented in Figure 4, right). Equation (B.5) for the contour of S_p

becomes

$$x_2 = a \cos^3 \varphi - D \sin \varphi \operatorname{sign}(\sin 2\varphi), \quad y_2 = a \sin^3 \varphi - D \cos \varphi \operatorname{sign}(\sin 2\varphi)$$

where

$$\begin{aligned} \varphi_D \leq \varphi \leq \pi/2 - \varphi_D, \quad \pi/2 + \varphi_D \leq \varphi \leq \pi - \varphi_D, \\ \pi + \varphi_D \leq \varphi \leq 3\pi/2 - \varphi_D, \quad 3\pi/2 + \varphi_D \leq \varphi \leq 2\pi - \varphi_D. \end{aligned}$$

$\varphi_D(t)$ is the parameter determining the size of the region S_p and $0 < \varphi_D \leq \pi/4$. The regions S_p and Z_2 are not present if $\varphi_D = \pi/4$.

Equations (20), (21), (23) for mechanism 2 of the astroid-shaped plate in the absence of resistance foundation look like

$$\rho \ddot{\alpha}(\Sigma_1 + \Sigma_2) = P(t)(\Sigma_3 + \Sigma_4) - M_0(2 - \eta)\Sigma_5, \tag{25}$$

$$\rho(\dot{\alpha}D)' = P(t), \tag{26}$$

$$D = \Sigma_6. \tag{27}$$

Here

$$\begin{aligned} \Sigma_1(\varphi_D) &= \iint_{Z_1} v_1^2 ds = 8 \int_0^{\varphi_D} \left[\int_0^{D_h(v_2)} v_1^2 F(v_1, v_2) dv_1 \right] dv_2 \\ &= \frac{2a^4}{3} \left(\frac{\sin^{11} \varphi_D}{\cos^3 \varphi_D} + \frac{\sin^9 \varphi_D}{\cos \varphi_D} + \frac{9}{8} \sin^7 \varphi_D \cos \varphi_D + \frac{63}{48} \sin^5 \varphi_D \cos \varphi_D \right. \\ &\quad \left. + \frac{315}{192} \sin^3 \varphi_D \cos \varphi_D - \frac{315}{128} (\varphi_D - \sin \varphi_D \cos \varphi_D) \right), \end{aligned}$$

$$\Sigma_2(\varphi_D) = \iint_{Z_2} v_1^2 ds = 8 \int_{\varphi_D}^{\pi/4} \left[\int_0^D v_1^2 F(v_1, v_2) dv_1 \right] dv_2$$

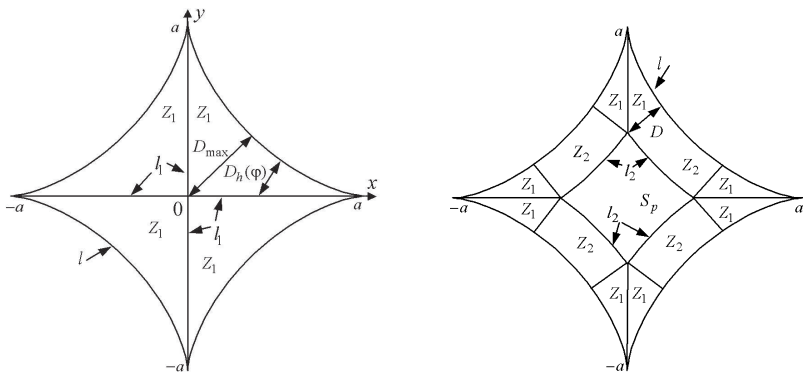


Figure 4. Mechanism 1 (left) and 2 (right) for astroid-shaped plate (the positions of the coordinate axes on the right are the same as those on the left).

$$= \frac{2a^4 \sin^9 \varphi_D}{\cos^3 \varphi_D} \left[\frac{\sin^3 \varphi_D}{\cos \varphi_D} (\pi/4 - \varphi_D) + 1 - 2 \sin^2 \varphi_D \right],$$

$$\begin{aligned} \Sigma_3(\varphi_D) &= \iint_{Z_1} v_1 ds = 8 \int_0^{\varphi_D} \left[\int_0^{D_h(v_2)} v_1 F(v_1, v_2) dv_1 \right] dv_2 \\ &= \frac{4a^3}{3} \left(\frac{\sin^{10} \varphi_D}{\cos^2 \varphi_D} + \sin^8 \varphi_D - \frac{\sin^6 \varphi_D}{6} - \frac{\sin^4 \varphi_D}{4} - \frac{\sin^2 \varphi_D}{2} - \ln \cos \varphi_D \right), \end{aligned}$$

$$\begin{aligned} \Sigma_4(\varphi_D) &= \iint_{Z_2} v_1 ds = 8 \int_{\varphi_D}^{\pi/4} \left[\int_0^D v_1 F(v_1, v_2) dv_1 \right] dv_2 \\ &= \frac{2a^3 \sin^6 \varphi_D}{3 \cos^2 \varphi_D} \left[\frac{4 \sin^3 \varphi_D}{\cos \varphi_D} (\pi/4 - \varphi_D) + 9 \left(\frac{1}{2} - \sin^2 \varphi_D \right) \right], \end{aligned}$$

$$\Sigma_5 = \int_l dl = 8 \int_0^{\pi/4} L(\varphi) d\varphi = 6a,$$

$$\Sigma_6(\varphi_D) = a \sin^3 \varphi_D / \cos \varphi_D,$$

where $F(v_1, v_2) = v_1 + 3a \sin v_2 \cos v_2$.

If $0 < P_{\max} \leq P_0$ (low loads), the plate remains undeformed. We determine the limit load P_0 from Equation (25) at the moment t_0 of the beginning of the deformation (24) and from the condition $\ddot{\alpha}(t_0) = 0$,

$$P_0 = \min_{0 < \varphi_D \leq \pi/4} \frac{M_0(2 - \eta) \Sigma_5}{\Sigma_3 + \Sigma_4} = \frac{M_0(2 - \eta) \Sigma_5}{\Sigma_3(\pi/4)} \approx 32.55 \frac{M_0(2 - \eta)}{a^2}.$$

Thus the region S_p degenerates into a point which is the center of the coordinates.

If $P_0 < P_{\max} \leq P_1$ (moderate loads), where P_1 is the load under which the region S_p appears, the plate is deformed in accordance with mechanism 1. We determine the load P_1 as follows. From (25), (26) we eliminate $\ddot{\alpha}$. As a result, we have

$$-\frac{\rho \dot{\alpha} \dot{D}}{D} (\Sigma_1 + \Sigma_2) = P(t) \left[\Sigma_3 + \Sigma_4 - \frac{\Sigma_1 + \Sigma_2}{D} \right] - M_0(2 - \eta) \Sigma_5. \tag{28}$$

Taking into account that the relations

$$\dot{\alpha}(t_0) = 0, \quad P_1 = P(t_0), \quad \varphi_D(t_0) = \pi/4, \quad D(t_0) = a/2$$

hold if the region S_p appears at the initial time t_0 whereas the regions S_p and Z_2 are absent, we obtain from (28) that

$$P_1 = \frac{M_0(2 - \eta) \Sigma_5}{\Sigma_3(\pi/4) - \frac{2}{a} \Sigma_1(\pi/4)} \approx 63.33 \frac{M_0(2 - \eta)}{a^2}.$$

For moderate loads, the plate motion is governed by the Equation (25) for $\varphi_D = \pi/4$, which becomes

$$\ddot{\alpha}(t) = G[P(t) - P_0] \tag{29}$$

where $G = \Sigma_3(\pi/4)/[\rho\Sigma_1(\pi/4)]$. The initial conditions have the form (24). The load is removed at the time $t = T$, and the plate moves inertially for certain time.

For $t_0 \leq t \leq T$, integrating Equation (29), we have

$$\dot{\alpha}(t) = G \left[\int_{t_0}^t P(\tau) d\tau - P_0(t - t_0) \right], \quad \alpha(t) = G \left[\int_{t_0}^t \int_{t_0}^m P(\tau) d\tau dm - P_0 \frac{(t - t_0)^2}{2} \right].$$

At $T < t \leq t_f$, the motion of the plate occurs due to inertia until the plate stops at the time t_f and it is governed by the equation $\ddot{\alpha}(t) = -GP_0$ with the initial conditions $\dot{\alpha}(T), \alpha(T)$. The moment t_f is determined by the condition

$$\dot{\alpha}(t_f) = 0. \tag{30}$$

Integrating the equation of motion, we obtain

$$\begin{aligned} \dot{\alpha}(t) &= \dot{\alpha}(T) - GP_0(t - T), \\ \alpha(t) &= \alpha(T) + \dot{\alpha}(T)(t - T) - GP_0(t - T)^2/2. \end{aligned} \tag{31}$$

It follows Equations (30), (31) that

$$t_f = t_0 + \int_{t_0}^T P(t) dt / P_0. \tag{32}$$

The deflections are calculated from (8) or (10). The maximum final deflection is in the center of the plate and it is

$$w_{\max} = D_{\max} G \left[\left(\int_{t_0}^T P(t) dt \right)^2 / (2P_0) - \int_{t_0}^T (t - t_0) P(t) dt \right]. \tag{33}$$

If $P_{\max} > P_1$ (high loads), the plate motion begins with the developed region S_p and $\varphi_0 = \varphi_D(t_0)$ which is less than $\pi/4$. The initial value φ_0 is determined by Equation (28) with the equality $\dot{\alpha}(t_0) = 0$ and the relation (27):

$$P_{\max} \left[\Sigma_3(\varphi_0) + \Sigma_4(\varphi_0) - \frac{\Sigma_1(\varphi_0) + \Sigma_2(\varphi_0)}{\Sigma_6(\varphi_0)} \right] = M_0(2 - \eta)\Sigma_5. \tag{34}$$

In the first phase ($t_0 < t \leq t_1$) of deformation, the plate motion occurs according to mechanism 2 and is described by Equations (22), (25)–(27) with the initial conditions (24) and (34). In this phase, the region S_p decreases by the law described by Equation (28). The time t_1 corresponding to the disappearance of the region S_p is determined by the equality $\varphi_D(t_1) = \pi/4$. At the end of this phase, the values of $\dot{\alpha}(t_1)$ and $\alpha(t_1)$ are determined.

The second phase ($t_1 < t \leq t_f$) of the plate motion occurs according to mechanism 1 until the stop at the time t_f . The deformation is governed by Equation (29) subject to the initial conditions determined at the end of the first phase. The time t_f is determined by (30). All deflections in the plate are calculated from (8) or (10) and (22) with allowance for all phases of motion.

In the case of high load represented by a rectangular pulse ($P(t) = P_{\max}$ for $t_0 \leq t \leq T$ and $P(t) = 0$ for $t > T$), the motion occurs with the constant region S_p during the action of the load ($t_0 \leq t \leq T$) and is described by Equations (22), (25)–(27) for $\varphi_D = \varphi_0$ determined from (34) with the initial conditions (24). After removal of the load, the second and the third phases of motion ($T < t \leq t_1$ and $t_1 < t \leq t_f$) occur.

They are described by the same equations in the first and second phases of motion of the plate under explosive loading but for the condition $P(t) = 0$.

The results of the deflections $w = ua^2\rho/(M_0T^2)$ of the simply supported astroid-shaped plate in the cross section $y = x$ are shown in Figure 5. Curves 1–3 correspond to the deflections of the plate under a high load of a rectangular pulse with $P_{\max} = 135.27M_0/a^2$ at the times $t = T, t = t_1 = 2.14T, t = t_f = 4.16T$, respectively. Curves 4–6 refer to the deflections of the plate under a high load with a linear decreasing ramp time ($P(t) = 310.28(T - t)M_0/a^2$ for $0 \leq t \leq T$ and $P(t) = 0$ for $t > T$) at the times $t = T, t = t_1 = 2.5T, t = t_f = 4.77T$, respectively. The numerical calculations show that

$$t_1 = I/P_1, \quad t_f = I/P_0, \tag{35}$$

where $I = \int_0^T P(t)dt$ is the full pulse of the load.

4. Dynamic behavior of a plate whose contour consists of two arcs of circle

As another example, we consider the dynamic behavior of the plate with a contour consisting of two arcs of circle of the radius R and the central corner 2γ (Figure 1, top left; Figure 6). For this plate, $v_1 = R - r_1, v_2 = \phi$ where (r_1, ϕ) is the polar coordinate system with the pole located in the point $x = 0, y = -R \cos \gamma$. We have

$$D_h(\varphi) = R[1 - \cos \varphi / \cos(\gamma - \varphi)], \quad D_{\max} = D_h(\gamma) = R(1 - \cos \gamma)$$

with $0 \leq \varphi \leq \gamma$ and $0 < \gamma \leq \pi/2$. Depending on the value of P_{\max} , two mechanisms of deformation are possible for this plate. Under moderate loads, the plate is deformed into two parts of a cone surface with the formation of the rectilinear plastic hinge line locating on the x -axis (mechanism 1 is presented in Figure 1, top left). Under high loads, the region S_p is formed in the central part of the plate. The region S_p moves translationally (mechanism 2 is presented in Figure 6). The contour of the region S_p consists of two arcs of circle of the radius $R - D$ and the central corner $2(\gamma - \varphi_D)$, where $\varphi_D(t)$ is the parameter determining the size of the region S_p ($0 < \varphi_D \leq \gamma$). At $\varphi_D = \gamma$, the regions S_p and Z_2 are not present.

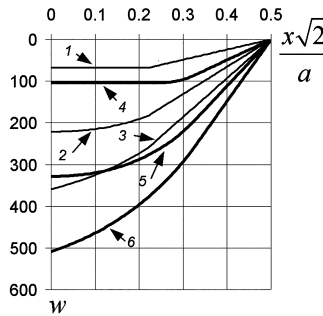


Figure 5. Deflections of a simply supported astroid-shaped plate in the cross section $x = y$.

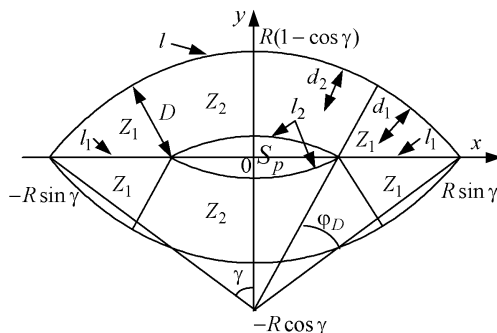


Figure 6. Mechanism 2 for the plate with a contour consisting of two arcs of a circle.

The equations of motion (20)–(23) for mechanism 2 of the plate being considered in the absence of resistance foundation look like (22), (25)–(27) where

$$\begin{aligned} \Sigma_1(\varphi_D) &= \iint_{Z_1} d_1^2 ds = 4 \int_0^{\varphi_D} \left[\int_{\frac{R \cos \gamma}{\cos(\gamma - \varphi)}}^R r_1 (R - r_1)^2 dr_1 \right] d\varphi \\ &= \frac{R^4}{3} \left\{ \varphi_D - 2 \cos^2 \gamma (3 + \cos^2 \gamma) [\operatorname{tg} \gamma - \operatorname{tg}(\gamma - \varphi_D)] \right. \\ &\quad \left. + 4 \cos^3 \gamma \left[\frac{\operatorname{tg} \gamma}{\cos \gamma} - \frac{\operatorname{tg}(\gamma - \varphi_D)}{\cos(\gamma - \varphi_D)} + \ln \frac{\cos \gamma [1 - \sin(\gamma - \varphi_D)]}{\cos(\gamma - \varphi_D)(1 - \sin \gamma)} \right] + \cos^4 \gamma \left[\frac{\sin(\gamma - \varphi_D)}{\cos^3(\gamma - \varphi_D)} - \frac{\sin \gamma}{\cos^3 \gamma} \right] \right\}, \\ \Sigma_2(\varphi_D) &= \iint_{Z_2} d_2^2 ds = 4 \int_0^{\gamma - \varphi_D} \left[\int_{R-D}^R r_1 (R - r_1)^2 dr_1 \right] d\varphi \\ &= \frac{(\gamma - \varphi_D) R^4}{3} \left[1 - \frac{\cos \gamma}{\cos(\gamma - \varphi_D)} \right]^3 \left[1 + \frac{3 \cos \gamma}{\cos(\gamma - \varphi_D)} \right], \\ \Sigma_3(\varphi_D) &= \iint_{Z_1} d_1 ds = 4 \int_0^{\varphi_D} \left[\int_{\frac{R \cos \gamma}{\cos(\gamma - \varphi)}}^R r_1 (R - r_1) dr_1 \right] d\varphi = \frac{2R^3}{3} \left\{ \varphi_D - \cos^2 \gamma [2 \operatorname{tg} \gamma - 3 \operatorname{tg}(\gamma - \varphi_D)] \right. \\ &\quad \left. + \cos^3 \gamma \left[\ln \frac{\cos \gamma [1 - \sin(\gamma - \varphi_D)]}{\cos(\gamma - \varphi_D)(1 - \sin \gamma)} - \frac{\operatorname{tg}(\gamma - \varphi_D)}{\cos(\gamma - \varphi_D)} \right] \right\}, \\ \Sigma_4(\varphi_D) &= \iint_{Z_2} d_2 ds = 4 \int_0^{\gamma - \varphi_D} \left[\int_{R-D}^R r_1 (R - r_1) dr_1 \right] d\varphi \\ &= \frac{2(\gamma - \varphi_D) R^3}{3} \left[1 - \frac{\cos \gamma}{\cos(\gamma - \varphi_D)} \right]^2 \left[1 + \frac{2 \cos \gamma}{\cos(\gamma - \varphi_D)} \right], \end{aligned}$$

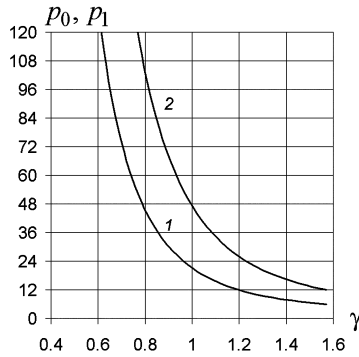


Figure 7. Dimensionless loads p_0 (curve 1) and p_1 (curve 2) for plate with a contour consisting of two arcs of a circle.

$$\Sigma_5 = \int_l dl = 4\gamma R,$$

$$\Sigma_6(\varphi_D) = R[1 - \cos \gamma / \cos(\gamma - \varphi_D)].$$

The analysis of the dynamic behavior of the plate being considered is similar to the analysis performed above for the astroid-shaped plate. We present some results. The limit load is calculated by the formula

$$\begin{aligned} P_0 &= \min_{0 < \varphi_D \leq \gamma} \frac{M_0(2 - \eta)\Sigma_5}{\Sigma_3 + \Sigma_4} = \frac{M_0(2 - \eta)\Sigma_5}{\Sigma_3(\gamma)} \\ &= \frac{M_0(2 - \eta)}{R^2} \frac{6\gamma}{\gamma - \sin 2\gamma + \cos^3 \gamma \ln[\cos \gamma / (1 - \sin \gamma)]}. \end{aligned} \tag{36}$$

The load P_1 under which the region S_p appears is found by the formula

$$\begin{aligned} P_1 &= \frac{M_0(2 - \eta)\Sigma_5}{\Sigma_3(\gamma) - \Sigma_1(\gamma)/D_{\max}} \\ &= \frac{12M_0(2 - \eta)\gamma}{R^2} \left/ \left[2 \left(\gamma - \sin 2\gamma + \cos^3 \gamma \ln \frac{\cos \gamma}{1 - \sin \gamma} \right) \right. \right. \\ &\quad \left. \left. - \frac{\gamma - 3 \sin \gamma \cos \gamma + 2 \cos^3 \gamma (2 \ln \frac{\cos \gamma}{1 - \sin \gamma} - \sin \gamma)}{1 - \cos \gamma} \right] \right. \end{aligned} \tag{37}$$

For the central corner $\gamma = \pi/2$, the plate being considered becomes a circular plate of the radius R . The limit load for it from the formula (36) is $P_0 = 6M_0(2 - \eta)/R^2$. In the simply supported case, this value is equal to the exact value of the limit load \bar{P}_0 obtained by Hopkins and Prager [1954]. For the clamped contour, the limit load from the formula (36) is equal to $2\bar{P}_0$. In [Florence 1966], it is obtained as a result of the approached decision using the Tresca yield criterion and is equal to $1.875\bar{P}_0$. For a circular plate, the formula (37) gives $P_1 = 2P_0$. In the simply supported case, this result coincides with those obtained by Hopkins and Prager [1954] and Perzyna [1958]. In the clamped case, Florence [1966] obtained that $P_1 = 1.998 \times 1.875\bar{P}_0 = 3.746\bar{P}_0$. Figure 7 shows the dimensionless loads p_0 and p_1 versus

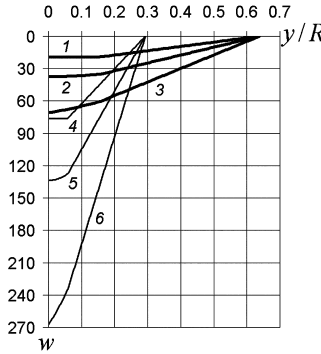


Figure 8. Deflections of a simply supported plate with a contour consisting of two arcs of a circle in the cross section $x = 0$.

the geometrical parameter γ ($p_i = P_i R^2 / [(2 - \eta) M_0]$, $i = 0, 1$). The curves 1, 2 correspond to the loads p_0, p_1 , respectively.

For moderate loads, the final deflection in the center of the plate being considered is calculated from the formula (33) $G = \Sigma_3(\gamma) / [\rho \Sigma_1(\gamma)]$.

The results of the deflections $w = u R^2 \rho / (M_0 T^2)$ of the simply supported plate being considered in the cross section $x = 0$ are in Figure 8. The plate is subjected to a high load represented by rectangular pulse $P(t) = P_m M_0 / R^2$ for $0 \leq t \leq T$ and $P(t) = 0$ for $t > T$. Curves 1–3 correspond to the deflections of the plate with $\gamma = 1, 2, D_{\max} = 0.638R$ and $P_m = 38.37$ at the times $t = T, t = t_1 = 1.48T, t = t_f = 3.22T$, respectively. Curves 4–6 correspond to the deflections of the plate with $\gamma = \pi/4, D_{\max} = 0.293R$ and $P_m = 152.22$ at the times $t = T, t = t_1 = 1.38T, t = t_f = 3.13T$, respectively. As in the case of the astroid plate, the numerical calculations show that the equalities (35) are valid.

For circular simply supported plate ($\gamma = \pi/2, \eta = 1$), the final deflection and the duration of response obtained by the offered method coincide with the result obtained by Perzyna [1958] and Youngdahl [1971].

By the method described in the present work, we analyzed an astroid-shaped plate and a plate with a contour consisting of two arches of circle under explosive loads represented by the various form of a pulse in the absence of resistance foundation. All calculations show that the equalities (35) are valid. In addition, it is established that the plates have the equal final deflections if different loads have two equal integral characteristics I and $I_* = \int_0^T t P(t) dt$. This property for the maximum final deflection is obtained analytically for rigid-plastic circular plates by Youngdahl [1971] and for regular polygonal plates by Nemirovsky and Romanova [1995].

5. Dynamic behavior of a plate with an internal free hole or a rigid insert

The previous result is easy to modify for the determination of the dynamic deformation of the plates of a smooth curvilinear convex contour l , having an internal hole l_2 which can be either free or clamped by an absolutely rigid insert, which is located at the identical distance D_a from the external contour. We assume that $D_a \leq D_{\min}$. The equation of the internal contour l_2 has the form (B.5) for $D = D_a$ (see Appendix B). We consider the following. By the action of the load $P(t)$, the plate is deformed into

a cone-shaped surface without the formation of the region of intense plastic deformation whereas the rigid insert and the points of the internal contour l_2 move translationally with the identical velocity $\dot{w}_c(t)$. Consequently, the angle of rotation of the plate surface around of the contour l is identical for all φ . Let us denote this angle by $\alpha(t)$.

Since, on the internal contour l_2 , the normal bending moment is equal to zero for the free contour and equal to M_0 for the case of a rigid insert, the power of internal forces is

$$N = \dot{\alpha}^* M_0 \left[(2 - \eta) \int_l dl - \beta \int_{l_2} dl \right], \tag{38}$$

where $\beta = 1$ for the case of a free hole and $\beta = 0$ for the plate with a rigid insert. We have

$$\int_l dl = \int_0^{2\pi} L(\varphi) d\varphi, \quad \int_{l_2} dl = \int_0^{2\pi} \sqrt{x'^2_2 + y'^2_2} d\varphi,$$

where $L(\varphi)$ is determined in (2). Taking into account the expression (B.5) for l_2 , we get

$$\int_{l_2} dl = \int_0^{2\pi} L(\varphi) d\varphi - D_a \int_0^{2\pi} \frac{L(\varphi)}{r(\varphi)} d\varphi.$$

Then the expression (38) for N becomes

$$N = \dot{\alpha}^* M_0 \left[(2 - \eta - \beta) \int_0^{2\pi} L(\varphi) d\varphi + D_a \beta \int_0^{2\pi} \frac{L(\varphi)}{r(\varphi)} d\varphi \right].$$

The expressions (6) look like

$$\begin{aligned} K &= \rho \dot{\alpha}^* \ddot{\alpha} \iint_{Z_2} v_1^2 ds + (1 - \beta) \rho_a \dot{w}_c^* \ddot{w}_c \iint_{S_p} ds, \\ A &= \dot{\alpha}^* \left[P(t) \iint_{Z_2} v_1 ds - (K_1 \alpha + K_2 \dot{\alpha}) \iint_{Z_2} v_1^2 ds \right] \\ &\quad + (1 - \beta) \dot{w}_c^* [P(t) - K_1 w_c - K_2 \dot{w}_2] \iint_{S_p} ds, \end{aligned}$$

where ρ_a is the surface density of the insert material. Substituting the expressions K, A, N into (5) and taking into account the condition (22) of continuity of the velocities at the contour l_2 for $D = D_a$, we obtain the equation of motion of the plate under consideration:

$$\begin{aligned} &(\rho \ddot{\alpha} + K_1 \alpha + K_2 \dot{\alpha}) \iint_{Z_2} v_1^2 ds + (1 - \beta) D_a^2 (\rho_a \ddot{\alpha} + K_1 \alpha + K_2 \dot{\alpha}) \iint_{S_p} ds \\ &= P(t) \left[\iint_{Z_2} v_1 ds + (1 - \beta) D_a \iint_{S_p} ds \right] - M_0 \left[(2 - \eta - \beta) \int_0^{2\pi} L(\varphi) d\varphi + D_a \beta \int_0^{2\pi} \frac{L(\varphi)}{r(\varphi)} d\varphi \right]. \end{aligned} \tag{39}$$

The initial conditions look like (24).

We determine the limit load P_0 from (39), (24) and $\ddot{\alpha}(t_0) = 0$. Then, we have

$$P_0 = M_0 \left[(2 - \eta - \beta) \int_0^{2\pi} L(\varphi) d\varphi + D_a \beta \int_0^{2\pi} \frac{L(\varphi)}{r(\varphi)} d\varphi \right] / \left[\iint_{Z_2} v_1 ds + (1 - \beta) D_a \iint_{S_p} ds \right].$$

In the case of an annular plate of radius R with a free internal contour ($\beta = 1$), the limit load is

$$P_0 = \frac{6M_0(1 - \eta + D_a/R)}{D_a^2(3 - 2D_a/R)}.$$

For the simply supported external contour, this result coincides with that obtained by Grigoriev [1953]. For the clamped external contour, this limit load for various D_a/R exceeds the result calculated by Grigoriev [1953] by approximately 7%.

Equation (39) is an ordinary differential equation of 2-nd order with constant coefficients and a variable right part. Methods of solution of the Cauchy problem for such equations are well-known.

We determine the solution of the problem in the case of a free internal hole ($\beta = 1$) and in the absence of resistance foundation ($K_1 = K_2 = 0$). Then Equation (39) becomes (29) for $G = G_1$ where

$$G_1 = \iint_{Z_2} v_1 ds / \left(\rho \iint_{Z_2} v_1^2 ds \right).$$

Therefore, the analysis of the behavior of the plate being considered is similar to the analysis of the behavior of the plate under a moderate load, which is performed above in the part 3, for $G = G_1$ and $D_{\max} = D_a$. The moment that the plate comes to rest is determined by (32). The final deflection on the contour l_2 is calculated from (33). For an annular plate with the simply supported external contour, this result coincides with that obtained by Mroz [1958] for a moderate load.

6. Conclusions

A rigid-plastic model is applied to study the dynamic behavior of simply supported or clamped plates of arbitrary piecewise smooth curvilinear contour under uniformly distributed short-time intensive loads on visco-elastic foundation. Several mechanisms of the dynamic deformation of the plates are considered. For each mechanism, equations of the dynamic deformation are derived. Operating conditions of these mechanisms are analyzed. The equations for the plastic hinge lines in the plate are obtained. A curvilinear orthogonal coordinate system in which double integrals in the equations of motion can be conveniently calculated is proposed. Analytical expressions for the limit and high loads and the maximum final deflections are obtained. Detailed analyses are given for an astroid-shaped plate and for the plate with a contour consisting of two arcs of circle. The calculations show that the fact that different explosive loads having two equal integral characteristics I and I_* is responsible for the identical final deflections of the plates. The governing equations for the behavior of a plate with an internal free hole or a rigid insert are obtained on analytically solvable form and details of the behavior are studied.

Appendix A

We show that the line normal to the curve l_2 is also the normal to the contour l . We approximate the curvilinear contour l by polygonal contour \bar{l} . For the polygonal plate obtained, the contour of the internal region which moves translationally becomes a polygonal contour \bar{l}_2 . Nemirovsky and Romanova [1987; 1988] showed that segments of the internal contour \bar{l}_2 are parallel to the corresponding segments of an external contour \bar{l} and line normal to any segments of \bar{l}_2 is also normal to corresponding side of \bar{l} . Hence, as the number of segments of the polygonal contour \bar{l} tends to be infinity, the contour \bar{l}_2 comes closer and closer to l_2 , and the normal to the curve l_2 at any point of l_2 is also a normal to the contour l .

Appendix B

Let us consider any smooth part of the contour l . We draw the normal to the curve l_2 from point $(x_2, y_2) \in l_2$ so that it intersects l at point $(x_1, y_1) \in l$. The distance between curves l and l_2 is written as $D = \delta r$, where $r(\varphi)$ is the radius of curvature of the curve l and $\delta = \delta(\varphi, t) \geq 0$ is a dimensionless function. The equation for the curve l_2 has the form

$$x_2 = x_1 - \delta(x_1 - \xi), \quad y_2 = y_1 - \delta(y_1 - \varsigma).$$

Here ξ, ς are the coordinates of the center of curvature of the curve l :

$$\xi = x_1 - \frac{y_1' L^2}{x_1' y_1'' - y_1' x_1''}, \quad \varsigma = y_1 + \frac{x_1' L^2}{x_1' y_1'' - y_1' x_1''},$$

where $L(\varphi)$ is given in (2)

Then the equations for the curve l_2 look like

$$x_2 = x_1 - \delta \frac{y_1' L^2}{x_1' y_1'' - y_1' x_1''}, \quad y_2 = y_1 + \delta \frac{x_1' L^2}{x_1' y_1'' - y_1' x_1''}. \tag{B.1}$$

As the normal to the contour l is also the normal to l_2 (Appendix A), we obtain

$$x_2'(x_2 - x_1) + y_2'(y_2 - y_1) = 0, \quad x_1'(x_1 - x_2) + y_1'(y_1 - y_2) = 0.$$

These relations yield

$$x_2' y_1' = y_2' x_1'. \tag{B.2}$$

Differentiating (B.1) and substituting the resulting relations into (B.2), we arrive at the differential equation for the function $\delta(\varphi, t)$

$$\delta' \frac{L^4}{x_1' y_1'' - y_1' x_1''} + \delta \left\{ x_1' \left[\frac{x_1' L^2}{x_1' y_1'' - y_1' x_1''} \right]' + y_1' \left[\frac{y_1' L^2}{x_1' y_1'' - y_1' x_1''} \right]' \right\} = 0.$$

Taking into account the following relations

$$\begin{aligned} x_1' \left[\frac{x_1' L^2}{x_1' y_1'' - y_1' x_1''} \right]' + y_1' \left[\frac{y_1' L^2}{x_1' y_1'' - y_1' x_1''} \right]' &= (x_1' x_1'' + y_1' y_1'') \frac{L^2}{x_1' y_1'' - y_1' x_1''} + (x_1'^2 + y_1'^2) \left[\frac{L^2}{x_1' y_1'' - y_1' x_1''} \right]' \\ &= L L' \frac{L^2}{x_1' y_1'' - y_1' x_1''} + L^2 \left[\frac{L^2}{x_1' y_1'' - y_1' x_1''} \right]' \\ &= L \left[\frac{L^3}{x_1' y_1'' - y_1' x_1''} \right]', \end{aligned}$$

we obtain the solution of the equation for the function $\delta(\varphi, t)$:

$$\delta = \delta_0(x_1' y_1'' - y_1' x_1'')/L^3, \quad \delta_0 = \delta_0(t) \geq 0. \quad (\text{B.3})$$

The radius of curvature $r(\varphi)$ of the curve l has the form (1); then, it follows (B.3) that

$$D = \delta(\varphi, t)r(\varphi) = \delta_0(t). \quad (\text{B.4})$$

Consequently, the distance D between the curves l and l_2 is independent of the parameter φ . With (B.3), (B.4), (B.1) for l_2 becomes

$$x_2 = x_1 - D y_1' / L, \quad y_2 = y_1 + D x_1' / L. \quad (\text{B.5})$$

References

- [Erkhov 1978] M. I. Erkhov, *Theory of ideal plastic solids and structures*, Nauka, Moscow, 1978. (in Russian).
- [Florence 1965] A. L. Florence, "Annular plate loaded by a transverse linear pulse", *AIAA J.* **3**:9 (1965), 1726–1733.
- [Florence 1966] A. L. Florence, "Behavior of a clamped circular rigid-plastic plate under explosive pressure", *Trans ASME (Ser. E, J. Appl. Mech.)* **33**:2 (1966), 11–17.
- [Grigoriev 1953] A. S. Grigoriev, "On the load-carrying capacities of the annular plates", *Ingen. Sbornik* **16** (1953), 177–182. (in Russian).
- [Hopkins and Prager 1953] H. G. Hopkins and W. Prager, "The load-carrying capacities of circular plates", *J. Mech. Phys. Solids* **2**:1 (1953), 1–13.
- [Hopkins and Prager 1954] H. G. Hopkins and W. Prager, "On the dynamics of plastic circular plates", *Z. Angew. Math. Phys.* **5** (1954), 317–330.
- [Jones 1971a] N. Jones, "A theoretical study of the dynamic plastic behavior of beams and plates with finite-deflections", *Int. J. Solids Struct.* **7** (1971a), 1007–1029.
- [Jones 1971b] N. Jones, "Large deflection of rectangular plates", *J. Ship Res.* **15**:2 (1971b), 164–171.
- [Jones 1973] N. Jones, "Slamming damage", *J. Ship Res.* **17**:2 (1973), 80–86.
- [Jones and Shen 1993] N. Jones and W. Q. Shen, "Dynamic response and failure of fully clamped circular plates under impulsive loading", *Int. J. Impact Eng.* **13**:2 (1993), 259–278.
- [Jones et al. 1970] N. Jones, T. O. Uran, and S. A. Tekin, "The dynamic plastic behavior of fully clamped rectangular plates", *Int. J. Solids Struct.* **6**:2 (1970), 1499–1512.
- [Komarov and Nemirovsky 1984] K. L. Komarov and Y. V. Nemirovsky, *Dynamics of rigid-plastic structural elements*, Nauka, Novosibirsk, 1984. (in Russian).
- [Mazalov and Nemirovsky 1975] V. N. Mazalov and Y. V. Nemirovsky, "Dynamics of thin-walled plastic structures", pp. 155–247 in *Dynamic Problems of Plastic Media (ser. Mech.)*, vol. 5, 1975.
- [Mroz 1958] Z. Mroz, "Plastic deformations of annular plates under dynamic loads", *Arch. Mech. Stos.* **10** (1958), 499–516.

- [Nemirovsky and Romanova 1987] Y. V. Nemirovsky and T. P. Romanova, “Dynamic behavior of doubly connected polygonal plastic plates”, *Int. Appl. Mech.* **23**:5 (1987), 458–464.
- [Nemirovsky and Romanova 1988] Y. V. Nemirovsky and T. P. Romanova, “Dynamic bending of polygonal plastic slabs”, *J. Appl. Mech. Tech. Phys.* **29**:4 (1988), 591–597.
- [Nemirovsky and Romanova 1991] Y. V. Nemirovsky and T. P. Romanova, “Dynamics of polygonal plastic plates with rounded corners”, *Strength Mater. (Ukraine)* **32**:9 (1991), 62–66.
- [Nemirovsky and Romanova 1995] Y. V. Nemirovsky and T. P. Romanova, “Effect pulsed load form on final deformations of rigid-plastic plates of a complex form”, *J. Appl. Mech. Tech. Phys.* **36**:6 (1995), 113–121.
- [Nemirovsky and Romanova 2001a] Y. V. Nemirovsky and T. P. Romanova, “Dynamic plastic deformation of curvilinear plates”, *Int. Appl. Mech.* **37**:12 (2001a), 1568–1578.
- [Nemirovsky and Romanova 2001b] Y. V. Nemirovsky and T. P. Romanova, “Optimization of dynamic plastic deformation of plates with a complex contour”, *J. Appl. Mech. Tech. Phys.* **42**:1 (2001b), 152–159.
- [Nemirovsky and Romanova 2002a] Y. V. Nemirovsky and T. P. Romanova, “Dynamic plastic damage of simply and doubly connected elliptic plates”, *J. Appl. Mech. Tech. Phys.* **43**:2 (2002a), 291–301.
- [Nemirovsky and Romanova 2002b] Y. V. Nemirovsky and T. P. Romanova, “Modeling and analysis of pressing of thing-walled structures of smooth convex contours”, pp. 231–239 in *Mechanics of shells and plates, proc. XX int. conf. on theory of shells and plates*, Nizhnii Novgorod State University, 2002b. (in Russian).
- [Nemirovsky and Romanova 2002c] Y. V. Nemirovsky and T. P. Romanova, “Damage of plane barriers of nonconcave contours under explosive loads”, *Nauch. vestnik* **2** (2002c), 77–85. Novosibirsk State Technical University (in Russian).
- [Nemirovsky and Romanova 2004] Y. V. Nemirovsky and T. P. Romanova, “Dynamic behavior of rigid-plastic sector plates”, *Int. Appl. Mech.* **40**:4 (2004), 440–447.
- [Perzyna 1958] P. Perzyna, “Dynamic load carrying capacity of circular plate”, *Arch. Mech. Stos.* **10**:5 (1958), 635–647.
- [Rzhanitsyn 1982] A. R. Rzhanitsyn, *Structural mechanics*, Vysshaya Shkola, Moscow, 1982. (in Russian).
- [Virma 1972] E. Virma, “Dynamics of plastic rectangular plates”, *Uch. Zap. Tart. Univ.* **305** (1972), 289–299.
- [Youngdahl 1971] C. K. Youngdahl, “Influence of pulse on the final plastic deformation of a circular plate”, *Int. J. Solids Struct.* **7**:9 (1971), 1127–1142.
- [Zhu et al. 1994] L. Zhu, D. Faulkner, and A. D. Atkins, “The impact of rectangular plates made from strain-rate sensitive material”, *Int. J. Impact Eng.* **15**:3 (1994), 243–255.

Received 17 Apr 2006. Revised 11 May 2006. Accepted 3 Jul 2007.

TATIANA PAVLOVNA ROMANOVA: shulgin@itam.nsc.ru
Institute of Theoretical and Applied Mechanics of the Siberian Branch of the Russian Academy of Science,
Institutaskaia str., 4/1, Novosibirsk, 630090, Russia

YURI VLADIMIROVICH NEMIROVSKY: nemirov@itam.nsc.ru
Institute of Theoretical and Applied Mechanics of the Siberian Branch of the Russian Academy of Science,
Institutaskaia str., 4/1, Novosibirsk, 630090, Russia